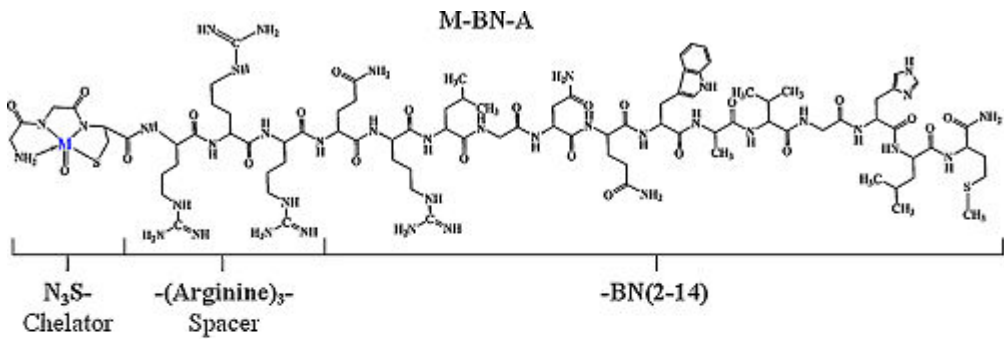
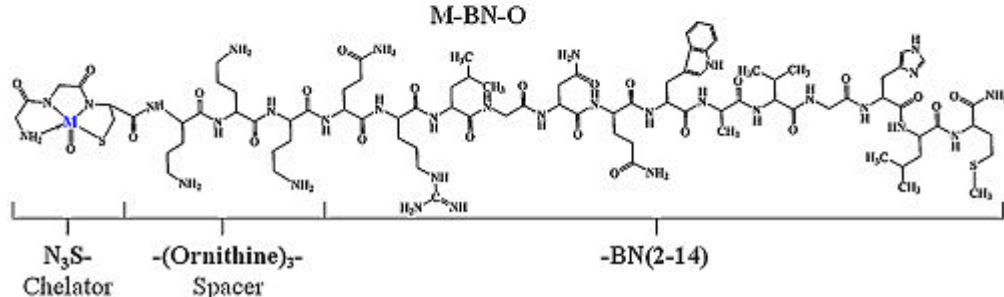


^{99m}Tc -Gly-Gly-Cys-(Arg)₃-bombesin(2-14)-NH₂

^{99m}Tc -BN-A

Liang Shan, PhD¹

Created: December 6, 2012; Updated: January 29, 2013.

Chemical name:	^{99m}Tc -Gly-Gly-Cys-(Arg) ₃ -bombesin(2-14)-NH ₂	 <p style="text-align: center;">M-BN-A</p>
Abbreviated name:	^{99m}Tc -BN-A	
Synonym:		
Agent Category:	Peptides	
Target:	Gastrin-releasing peptide receptors (GRPR)	
Target Category:	Receptors	
Method of detection:	Single-photon emission computed tomography (SPECT); gamma planar imaging	 <p style="text-align: center;">M-BN-O</p>
Source of signal / contrast:	^{99m}Tc	
Activation:	No	
Studies:	<ul style="list-style-type: none"> <i>In vitro</i> Rodents 	Structures of ^{99m}Tc -BN-A and ^{99m}Tc -BN-O (1).

¹ National Center for Biotechnology Information, NLM, NIH; Email: micad@ncbi.nlm.nih.gov.

[✉] Corresponding author.

Background

[PubMed]

^{99m}Tc -Gly-Gly-Cys-(Arg)₃-bombesin(2-14)-NH₂, abbreviated as ^{99m}Tc -BN-A, is an analog of the bombesin (BN) peptide, which was synthesized by Liolios et al. for imaging of tumors that express gastrin-releasing peptide receptors (GRPR) (1).

BN is an amphibian neuropeptide consisting of 14 amino acids (pGlu-Gln-Arg-Leu-Gly-Asn-Gln-Trp-Ala-Val-Gly-His-Leu-Met-NH₂) (2, 3). It shares an identical C-terminal region (-Trp-Ala-Val-Gly-His-Leu-Met-NH₂) with gastrin-releasing peptide (GRP), which is responsible for receptor binding and signal transduction (4, 5). There are three mammalian BN receptors, and GRPR (BB₂ or BRS2; 384 amino acids) is the only one that is well characterized. GRPR is a glycosylated, 7-transmembrane, G-protein-coupled receptor that, upon binding with its ligands, gives rise to a complex cascade of intracellular reactions. In the physiological state, GRPR is expressed at low levels in non-neuroendocrine tissues of the breast and pancreas, and in neuroendocrine cells of the brain, gastrointestinal tract, lung, and prostate (6). On the contrary, GRPR is overexpressed in various tumors, establishing itself as an optimal target for theranostics (7-10).

To date, a large number of BN derivatives have been synthesized based on either truncated BN(6-14) or BN(7-14) or full-length BN(1-14) (4, 10, 11). The truncated BN analogs are generally more stable *in vivo*, but the full-length analogs offer more flexible labeling sites through the amino acids 1 to 6. For most BN analogs, the amino acids on position 13 (Leu) and 14 (Met) have been replaced by unnatural amino acids, and Lys has been placed on position 3 for attachment of radiolabels. Spacers and chelators have also been widely used for conjugation purposes and for favorable kinetics.

In 2009, Fragogeorgi et al. reported two ^{99m}Tc -labeled BN derivatives with different hydrophilicities and overall charges (12). One BN derivative, ^{99m}Tc -N₃S-BN(2-14), had a sequence of $^{99m}\text{Tc}(\text{V})\text{O}$ -Gly-Gly-Cys-bombesin(2-14). Another BN derivative, ^{99m}Tc -BN-O or ^{99m}Tc -N₃S-X-BN(2-14), had the same sequence, but a basic amino acid spacer (X = Orn-Orn-Orn) was introduced. Both agents utilize the Gly-Gly-Cys as a tripeptide N₃S-type chelator for radiolabeling, but ^{99m}Tc -BN-O is more hydrophilic than ^{99m}Tc -N₃S-BN(2-14). Comparative studies have shown that hydrophilicity and charge strongly affect the binding properties and biodistribution patterns of the agents, and ^{99m}Tc -BN-O is superior to ^{99m}Tc -N₃S-BN(2-14) for use in imaging tumors. To understand whether presence of a positively charged and highly polar spacer is critical for body clearance, the same group of investigators recently developed the agent ^{99m}Tc -BN-A, which is a C-terminally amidated BN(2-14) analog with a positively charged, more polar natural spacer (Arg)₃ than the spacer (Orn)₃ (1). Liolios et al. investigated the *in vitro* and *in vivo* properties of ^{99m}Tc -BN-A and compared to the properties of ^{99m}Tc -BN-O (1). This chapter summarizes the comparative data obtained by Liolios et al. with ^{99m}Tc -BN-A and

^{99m}Tc -BN-O (1). The data obtained with ^{99m}Tc -N₃S-BN(2-14) and ^{99m}Tc -BN-O by Fragozeorgi et al. can be reviewed in the chapter on ^{99m}Tc -N₃S-X-BN(2-14) in MICAD.

Related Resource Links:

- [Protein, nucleotide \(RefSeq\), and gene information for GRPR](#)
- [Structure information of BN and analogs in PubChem](#)
- [GRPR-targeted imaging agents in MICAD](#)

Synthesis

[PubMed]

The BN peptides (Arg)₃-bombesin(2-14) (BN-A) and (Orn)₃-bombesin(2-14) (BN-O) were synthesized on a Rink-amide resin following the Fmoc strategy (1). The chemical purity for both BN-A and BN-O was >95%. Pure BN-A was obtained at a yield of ~39%, while introduction of the (Orn)₃ spacer in BN-O led to a significant reduction in yield (~9%). The two peptides presented a retention time (Rt) difference of 1.8 min in reverse-phase high-performance liquid chromatography (RP-HPLC), with BN-O eluting earlier than BN-A. ^{185/187}Re-A-BN and ^{185/187}Re-O-BN were prepared by ligand exchange reactions for 2 h at 67°C, starting from the ^{185/187}Re(V)O gluconate precursor. Radiolabeling with ^{99m}Tc was performed by radioisotope exchange from the ^{99m}Tc(V)O gluconate precursor for 30 min at 45°C. Sodium gluconate was used as an intermediate exchange ligand for ^{99m}Tc, and stannous chloride was used as a reducing agent. The radiochemical yield of both ^{99m}Tc-BN-A and ^{99m}Tc-BN-O was >98%. The stability for the two agents was tested up to 6 h after labeling, and both remained >90% intact. The Rts of ^{185/187}Re- and ^{99m}Tc-complexes were similar in RP-HPLC, indicating that ^{185/187}Re and ^{99m}Tc form complexes of similar structure. The specific activity was not reported.

The metabolic stability of ^{99m}Tc-BN-A and ^{99m}Tc-BN-O was studied in mouse plasma for 5, 15, 30, and 60 min at 37°C (1). Both agents presented similar metabolic patterns. After 5 min of incubation, 42.48 ± 1.45% of the ^{99m}Tc-BN-A and 44.28 ± 3.84% of the ^{99m}Tc-BN-O remained intact. One major radioactive metabolite for both agents was observed with Rt close to that of the corresponding intact peptides. This major metabolite probably contained a great part of the parent peptide chain, including the ^{99m}Tc-conjugated chelator group. After 1 h incubation, ~15% of the ^{99m}Tc-BN-A and ~18% of the ^{99m}Tc-BN-O remained intact.

The metabolic stability of ^{99m}Tc-BN-A and ^{99m}Tc-BN-O was also studied in human plasma for 1 h at 37°C (1). The metabolic patterns observed in human plasma were similar to the patterns observed in mouse plasma, but the peptide degradation in human plasma was much slower. At 1 h, 60.2 ± 1.2% of the ^{99m}Tc-BN-A and 63.0 ± 1.0% of the ^{99m}Tc-BN-O remained intact. A radioactive metabolite with Rt close to that of the intact peptide was also present for both agents, but in a smaller amount in comparison to the metabolite in mouse plasma. This metabolite was clearly visible in the mouse plasma after

the first 5 min of incubation, but 4%–5% was visible after 1 h incubation in the human plasma.

In Vitro Studies: Testing in Cells and Tissues

[PubMed]

The GRPR-binding capabilities (IC_{50} values) of BN-A, BN-O, and their $^{185/187}\text{Re}$ complexes were evaluated in GRPR-positive PC-3 cells with a competitive cell-binding assay, using [^{125}I -Tyr 4]-BN as the GRPR-specific radioligand and [Tyr 4]-BN as the control compound (1). Liolios et al. observed a typical sigmoid curve for displacement of [^{125}I -Tyr 4]-BN from PC-3 cells as a function of increasing concentration of all five different cold ligands under study (i.e., [Tyr 4]-BN, BN-A, BN-O, $^{185/187}\text{Re}$ -BN-A, and $^{185/187}\text{Re}$ -BN-O) (1). All compounds showed an affinity similar to that of the control peptide [Tyr 4]-BN (Table 1). Addition of the positively charged amino acid spacer and the Gly-Gly-Cys chelator group did not affect the binding affinity of the BN analogs. The differences for the receptor-binding affinity between BN-A and BN-O as well as between their $^{185/187}\text{Re}$ complexes were not significant.

Table 1. The IC_{50} values of the tested BN analogs.

Compound	IC_{50} (nM)	Standard error	Statistics
BN-A	0.50	0.09	N
$^{185/187}\text{Re}$ -BN-A	1.58	0.16	Y
BN-O	0.46	0.04	N
$^{185/187}\text{Re}$ -BN-O	0.77	0.07	Y
[Tyr 4]-BN	0.45	0.04	–

Y: statistical difference from [Tyr 4]-BN; N: no difference from [Tyr 4]-BN.

The uptake (internalization) and efflux (externalization), as a function of time of the $^{99\text{m}}\text{Tc}$ -BN-A and $^{99\text{m}}\text{Tc}$ -BN-O under study, were assessed with PC-3 cells in the presence (blocking experiments) or absence of the corresponding native BN peptides (1). The internalization rate of $^{99\text{m}}\text{Tc}$ -BN-A increased rapidly until 120 min after initialization of incubation with PC-3 cells. Between 90 min and 120 min, $^{99\text{m}}\text{Tc}$ -BN-A internalization reached a plateau and remained stable for >3 h of incubation. Nonspecific internalization in the presence of native BN was stable at <5% during the whole experiment. $^{99\text{m}}\text{Tc}$ -BN-O reached its plateau after the first 60 min of incubation. The specific and nonspecific internalization levels were similar for both agents.

The externalization rate was studied when the agents reached the maximum levels of internalization (1). Measurements up to 90 min after incubation showed that ~68% of the $^{99\text{m}}\text{Tc}$ -BN-A remained trapped in the cells, similar to measurements of the $^{99\text{m}}\text{Tc}$ -BN-O, indicating similar rates of externalization for both peptides.

Animal Studies

Rodents

[PubMed]

The biodistribution of ^{99m}Tc -BN-A and ^{99m}Tc -BN-O was comparatively studied in healthy female Swiss mice at 5, 15, 30, 60, 90, and 120 min, respectively, after injection of 2.775–4.625 MBq (0.075–0.125 mCi) of each agent *via* the tail vein (number of mice not reported) (1). Results were expressed as percentage of injected dose per organ (% ID/organ) or per gram tissue (% ID/g). Blood was assumed to be 7% of the total body weight for total blood radioactivity calculation. Receptor-blocking studies were carried out with co-administration of an excess amount (1 mg/ml) of the corresponding native BN peptides, and animals were euthanized at 30 min after co-injection.

Biodistribution studies showed that both agents cleared quickly from blood (1). ^{99m}Tc -BN-A had a higher blood value than ^{99m}Tc -BN-O (9.47 ± 1.12 versus $4.92 \pm 0.65\%$ ID/g) at 5 min after injection and exhibited a faster blood clearance thereafter, with lower blood concentrations than ^{99m}Tc -BN-O. The kinetic patterns of ^{99m}Tc -BN-A at 5 min after injection were similar in most organs, including heart, lungs, and liver, exhibiting higher values (% ID/g) than those of ^{99m}Tc -BN-O and rapidly decreasing thereafter. The uptake values of ^{99m}Tc -BN-A in lungs and liver were $8.91 \pm 0.87\%$ and $9.90 \pm 1.31\%$ ID/g at 5 min after injection, respectively, and $<5\%$ ID/g at 15 min in lungs and at 30 min in liver. ^{99m}Tc -BN-O remained $<5\%$ ID/g in lungs and liver during the whole experiment. The predominant excretion route for both agents was *via* the kidneys. The urine radioactivity for ^{99m}Tc -BN-A reached 63.34% ID/organ at 60 min after injection, while a similar value (63.15% ID/organ) was observed for ^{99m}Tc -BN-O at 120 min after injection. The ^{99m}Tc -BN-O urine value was 30.58% ID/organ at 60 min after injection. The high kidney retention for both agents was considered to be related to the increase in their overall charge due to the presence of positively charged amino acids in their spacer chains. In the GRPR-positive pancreas, ^{99m}Tc -BN-A exhibited a high uptake, with an initial value of $14.07 \pm 2.18\%$ ID/g and values of $>9.0\%$ ID/g until 120 min after injection. Accumulation for both agents peaked at $\sim 24.0\%$ ID/g in the pancreas at 15 min after injection. The uptake values in muscle, spleen, and stomach were insignificant for both agents.

The biodistribution of ^{99m}Tc -BN-A and ^{99m}Tc -BN-O was also studied in SCID mice bearing PC-3 tumors (number of mice not reported) (1). ^{99m}Tc -BN-A showed a high blood value at 15 min after injection ($7.14 \pm 1.4\%$ ID/g), which rapidly decreased within 60 min ($0.8 \pm 0.16\%$ ID/g). ^{99m}Tc -BN-A rapidly accumulated in the GRPR-positive PC-3 tumors ($6.94 \pm 0.50\%$ ID/g at 15 min after injection) and pancreas ($\sim 24\%$ ID/g at 15–30 min after injection). Blocking studies, performed at 30 min after co-administration of excess native BN, decreased accumulation of ^{99m}Tc -BN-A in the tumor and pancreas. The predominant excretion route of both ^{99m}Tc -BN-A and ^{99m}Tc -BN-O in the PC-3 tumor-bearing mice was also *via* the kidneys. For ^{99m}Tc -BN-A, the tumor/blood ratio increased until 120 min after injection, when it reached its highest value (4.53). The

tumor/muscle ratio, which was high already at 15 min after injection (4.74), reached its peak at 30 min (8.86), decreased at 60 min (5.60), and increased again at 120 min after injection (8.65). The tumor/intestine ratio presented its highest value at 15 min after injection (2.0) and then decreased gradually until 120 min after injection (1.25). The tumor/kidney and tumor/liver ratios presented similar and stable values, which were also decreased at 120 min after injection. ^{99m}Tc -BN-O presented a tumor/blood ratio of 1.86 at 30 min after injection, which increased to 33.32 at 120 min after injection. The tumor/kidney ratio was higher for ^{99m}Tc -BN-A at 60 min after injection and lower at 30 min and 120 min after injection (0.39, 0.27, and 0.28, respectively) than the respective ratios of ^{99m}Tc -BN-O (0.28, 0.52, and 0.48 at the same time points). The tumor/muscle ratio was higher for ^{99m}Tc -BN-A than for ^{99m}Tc -BN-O until 30 min after injection (8.86 *versus* 6.38) and decreased to values lower than those of ^{99m}Tc -BN-O thereafter. Tumor/liver ratios for ^{99m}Tc -BN-A were lower at all time points than the ratios for ^{99m}Tc -BN-O. Tumor/intestine ratios for ^{99m}Tc -BN-A were marginally higher than those for ^{99m}Tc -BN-O at 120 min after injection (1.25 *versus* 1.17), while for all other time points the ratios were lower.

Imaging studies were performed with γ -ray scintigraphy in PC-3 tumor-bearing mice at 120 min after injection of ~ 7.4 MBq (~ 0.2 mCi) ^{99m}Tc -BN-A (number of mice not reported) (1). The PC-3 tumor was visible as early as 10 min with clear contrast from the adjacent background and remained observable up to 60 min after injection. High radioactivity was observed in the kidneys and urinary bladder. Imaging analysis data were in agreement with the results obtained from the biodistribution study in PC-3 tumor-bearing mice.

Other Non-Primate Mammals

[PubMed]

No references are currently available.

Non-Human Primates

[PubMed]

No references are currently available.

Human Studies

[PubMed]

No references are currently available.

References

1. Liolios C.C., Fragogeorgi E.A., Zikos C., Loudos G., Xanthopoulos S., Bouziotis P., Paravatou-Petsotas M., Livaniou E., Varvarigou A.D., Sivolapenko G.B. *Structural modifications of (9)(9)mTc-labeled bombesin-like peptides for optimizing*

- pharmacokinetics in prostate tumor targeting*. Int J Pharm. 2012;430(1-2):1–17. PubMed PMID: 22459664.
2. Maina T., Nock B.A., Zhang H., Nikolopoulou A., Waser B., Reubi J.C., Maecke H.R. *Species differences of bombesin analog interactions with GRP-R define the choice of animal models in the development of GRP-R-targeting drugs*. J Nucl Med. 2005;46(5): 823–30. PubMed PMID: 15872357.
 3. Smith C.J., Volkert W.A., Hoffman T.J. *Gastrin releasing peptide (GRP) receptor targeted radiopharmaceuticals: a concise update*. Nucl Med Biol. 2003;30(8):861–8. PubMed PMID: 14698790.
 4. Smith C.J., Volkert W.A., Hoffman T.J. *Radiolabeled peptide conjugates for targeting of the bombesin receptor superfamily subtypes*. Nucl Med Biol. 2005;32(7):733–40. PubMed PMID: 16243649.
 5. Ananias H.J., de Jong I.J., Dierckx R.A., van de Wiele C., Helfrich W., Elsinga P.H. *Nuclear imaging of prostate cancer with gastrin-releasing-peptide-receptor targeted radiopharmaceuticals*. Curr Pharm Des. 2008;14(28):3033–47. PubMed PMID: 18991717.
 6. Weber H.C. *Regulation and signaling of human bombesin receptors and their biological effects*. Curr Opin Endocrinol Diabetes Obes. 2009;16(1):66–71. PubMed PMID: 19115523.
 7. Yang Y.S., Zhang X., Xiong Z., Chen X. *Comparative in vitro and in vivo evaluation of two 64Cu-labeled bombesin analogs in a mouse model of human prostate adenocarcinoma*. Nucl Med Biol. 2006;33(3):371–80. PubMed PMID: 16631086.
 8. Liu S., Edwards D.S., Barrett J.A. *99mTc labeling of highly potent small peptides*. Bioconjug Chem. 1997;8(5):621–36. PubMed PMID: 9327124.
 9. Zhang X., Cai W., Cao F., Schreibmann E., Wu Y., Wu J.C., Xing L., Chen X. *18F-labeled bombesin analogs for targeting GRP receptor-expressing prostate cancer*. J Nucl Med. 2006;47(3):492–501. PubMed PMID: 16513619.
 10. Schroeder R.P., van Weerden W.M., Bangma C., Krenning E.P., de Jong M. *Peptide receptor imaging of prostate cancer with radiolabelled bombesin analogues*. Methods. 2009;48(2):200–4. PubMed PMID: 19398012.
 11. Hohne A., Mu L., Honer M., Schubiger P.A., Ametamey S.M., Graham K., Stellfeld T., Borkowski S., Berndorff D., Klar U., Voigtmann U., Cyr J.E., Friebe M., Dinkelborg L., Srinivasan A. *Synthesis, 18F-labeling, and in vitro and in vivo studies of bombesin peptides modified with silicon-based building blocks*. Bioconjug Chem. 2008;19(9): 1871–9. PubMed PMID: 18754574.
 12. Fragogeorgi E.A., Zikos C., Gourni E., Bouziotis P., Paravatou-Petsotas M., Loudos G., Mitsokapas N., Xanthopoulos S., Mavri-Vavayanni M., Livaniou E., Varvarigou A.D., Archimandritis S.C. *Spacer site modifications for the improvement of the in vitro and in vivo binding properties of (99m)Tc-N(3)S-X-bombesin[2-14] derivatives*. Bioconjug Chem. 2009;20(5):856–67. PubMed PMID: 19344122.